Supporting Information

for

pH- and Redox-Triggered Synergistic Controlled Release of ZnO-Gated Hollow Mesoporous Silica Drug Delivery System

Shanshan Wu, Xuan Huang and Xuezhong Du*

Key Laboratory of Mesoscopic Chemistry (Ministry of Education), School of Chemistry and Chemical Engineering, Nanjing University, Nanjing 210093, People's Republic of China

E-mail: xzdu@nju.edu.cn

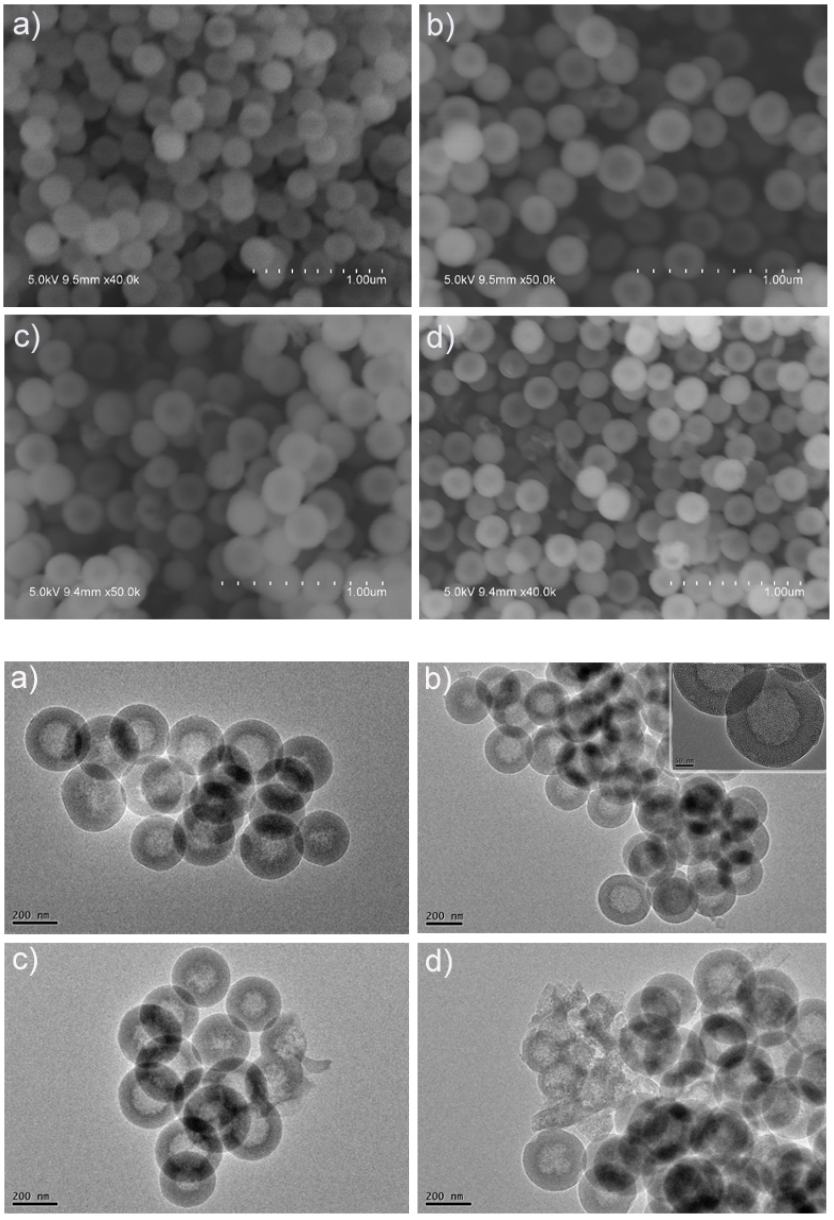

Fig. S1 SEM (top) and TEM (bottom) images of (a) HMSS10, (b) HMSS12, (c) HMSS14, and (d) HMSS16. Inset shows a magnification TEM image.

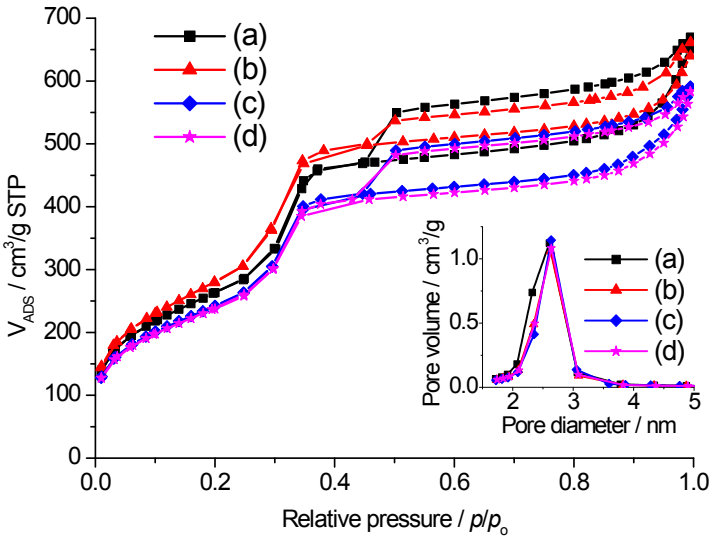

Fig. S2 Nitrogen adsorption–desorption isotherms and pore size distributions of (a) HMSS10, (b) HMSS12, (c) HMSS14, and (d) HMSS16.

Table S1 Specific surface area and average pore size of the HMSS materials based on the Brunauer–Emmett–Teller (BET) adsorption.

materials	surface area (m^2/g)	pore size (nm)
HMSS10	967	2.6
HMSS12	1029	2.6
HMSS14	887	2.6
HMSS16	870	2.6
APTMS-modified HMSS12	749	2.0
HMSS12-S-S-COOH	661	2.0

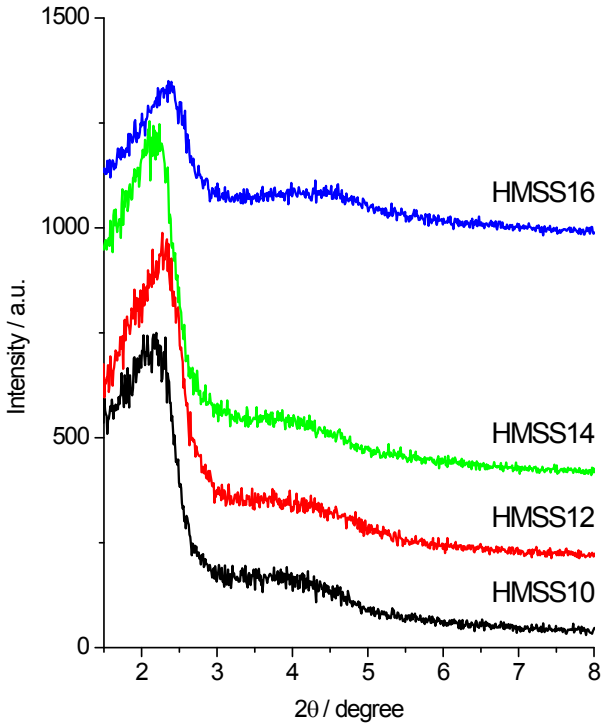

Fig. S3 Small-angle powder XRD patterns of HMSS10, HMSS12, HMSS14, and HMSS16.

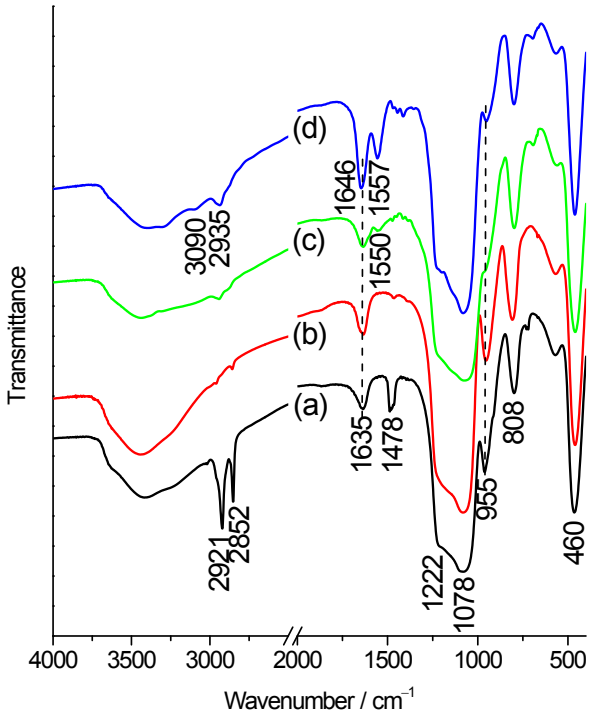

Fig. S4 FTIR spectra of (a) HMSS12 before removal of CTAB, (b) HMSS12, (c) APTMS-modified HMSS12, and (d) HMSS12-S-S-COOH.

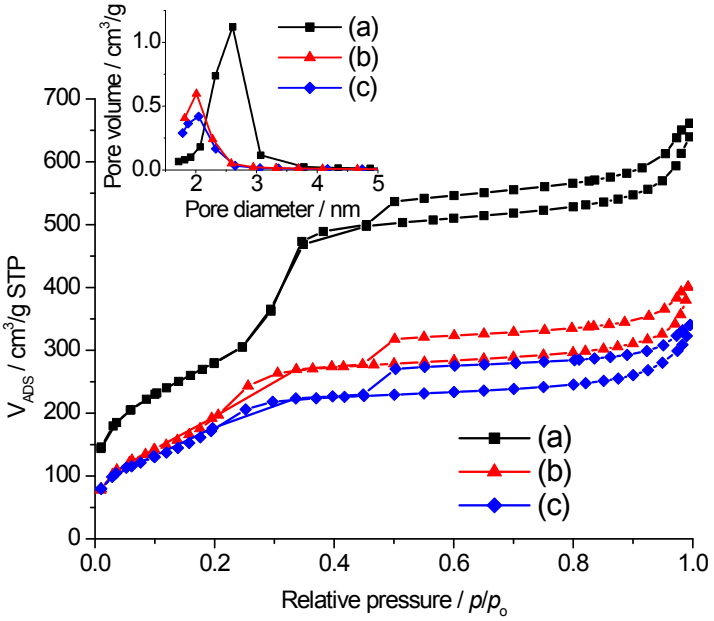

Fig. S5 Nitrogen adsorption–desorption isotherms and pore size distributions of (a) HMSS12, (b) APTMS-modified HMSS12, and (c) HMSS12-S-S-COOH.

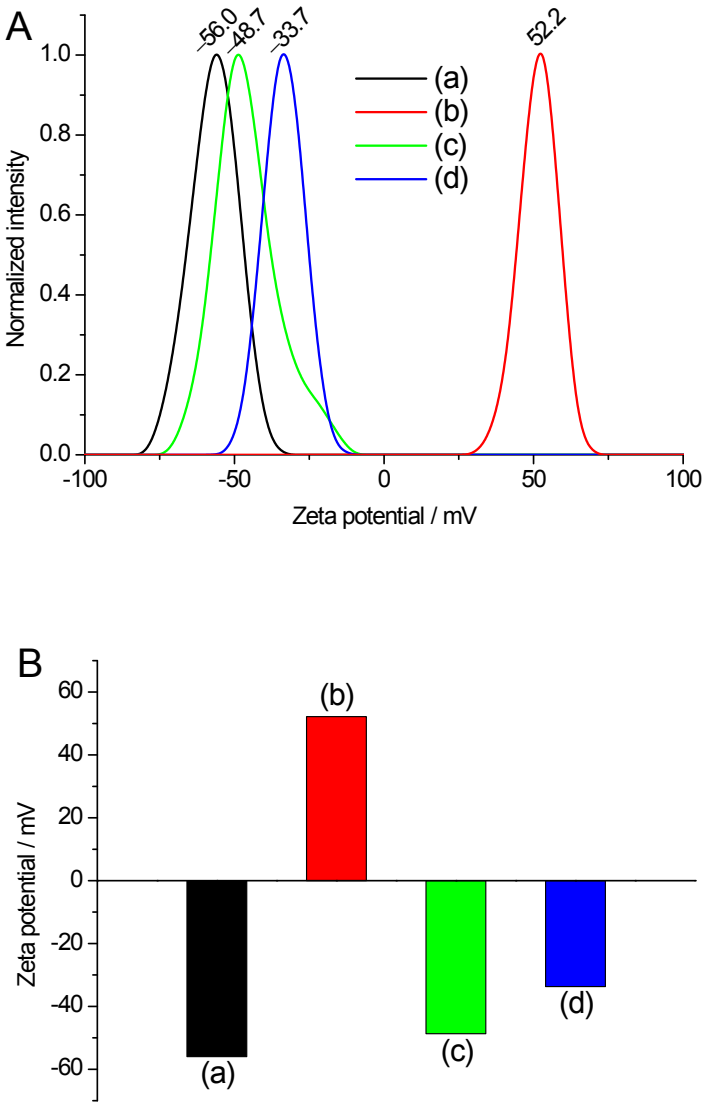

Fig. S6 Zeta potentials of (a) HMSS12, (b) APTMS-modified HMSS12, (c) HMSS12-S-S-COOH, and (d) ZnO-capped HMSS12 presented in different forms A and B.

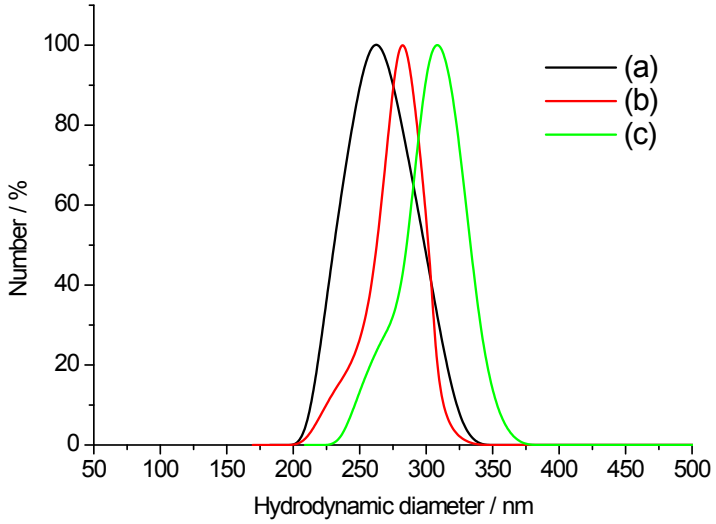

Fig. S7 Hydrodynamic diameter distributions of (a) HMSS12, (b) HMSS12-S-S-COOH, and (c) ZnO-capped HMSS12.

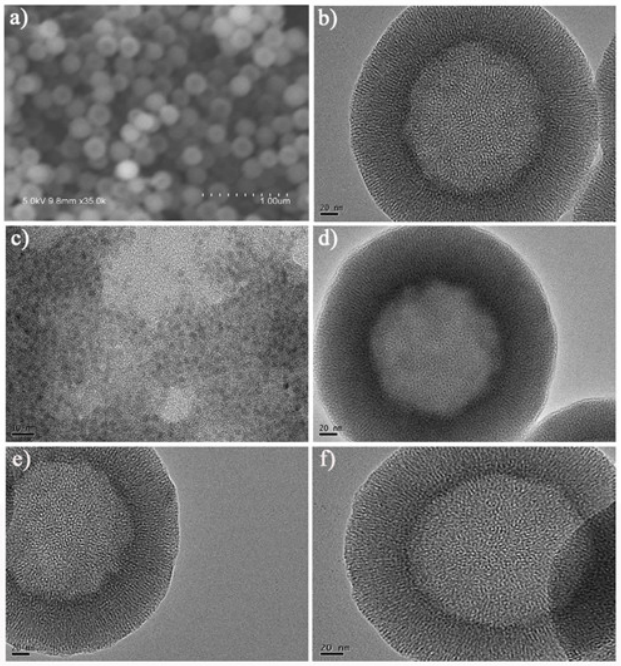

Fig. S8 (a) SEM and (b) TEM images of HMSS12-S-S-COOH and TEM images of (c) aminated ZnO QDs, (d) ZnO-capped HMSS12, (e) ZnO-capped HMSS12 after trigger of pH in the HEPES buffer solution at pH 5.0, and (f) ZnO-capped HMSS12 after trigger of GSH (10 mM) in the HEPES buffer solution at pH 7.4.

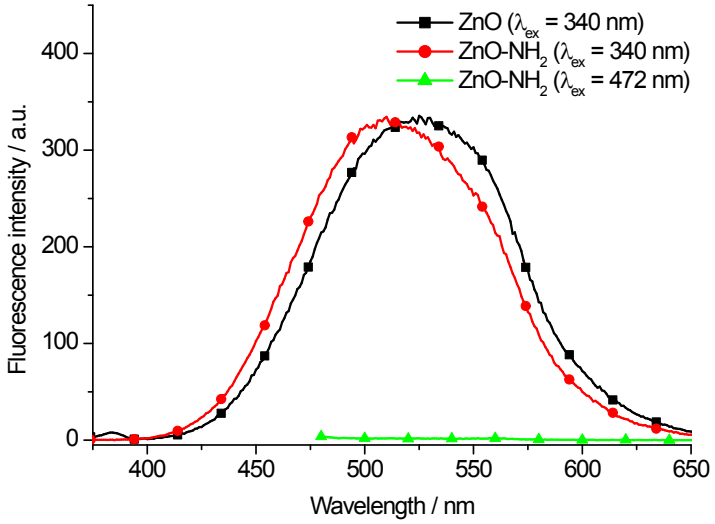

Fig. S9 Fluorescence spectra of (a) ZnO QDs, (b) aminated ZnO QDs at the excitation wavelength of 340 nm, and (c) aminated ZnO QDs at the excitation wavelength of 472 nm.

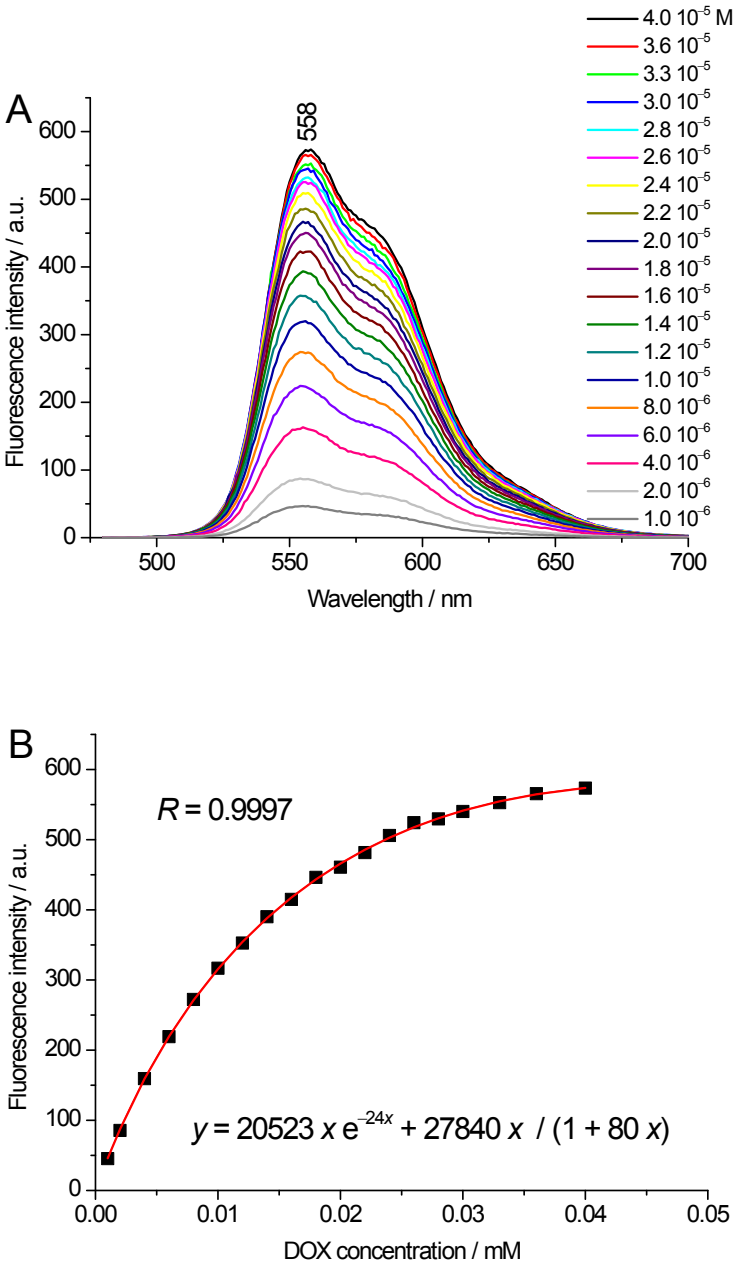

Fig. S10 (A) Fluorescence spectra of DOX in HEPES buffer solutions (pH 7.4) with different concentrations. (B) Emission intensity at 558 nm as a function of DOX concentration. (C) Fluorescence spectrum of final washing solution containing unloaded DOX in 40 mL of HEPES buffer solution from the ZnO-capped HMSS12 system.

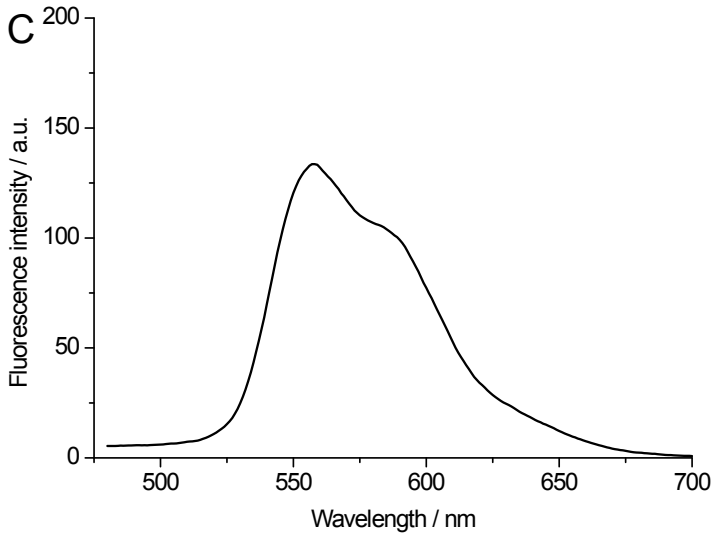

Fig. S10 (continued)

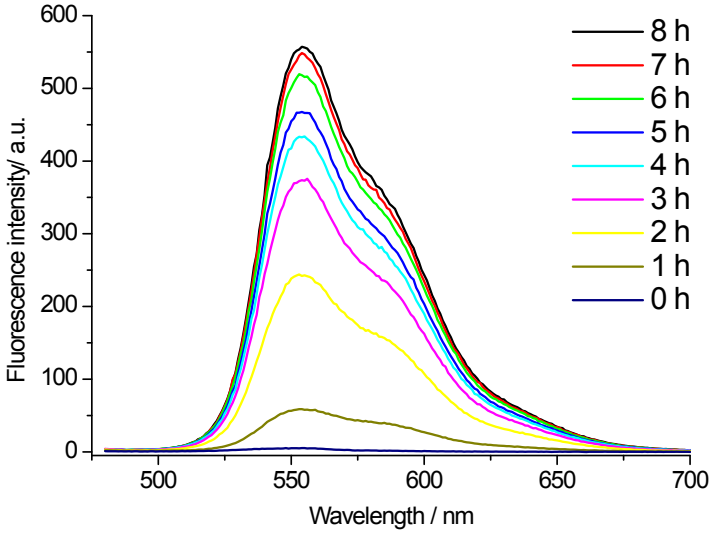

Fig. S11 pH-triggered time-dependent fluorescence spectra of DOX released from the ZnO-gated HMSS12 system in the HEPES buffer solution at pH 3.0 at the excitation wavelength of 472 nm.

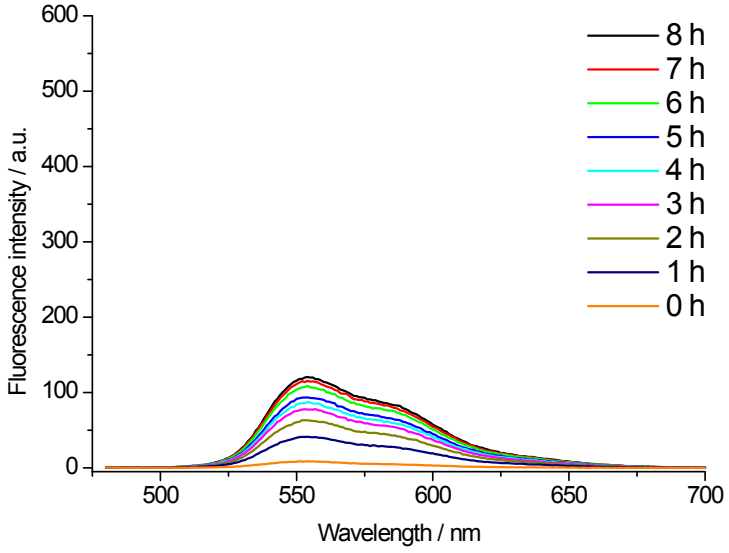

Fig. S12 pH-triggered time-dependent fluorescence spectra of DOX released from the HMSS system without ZnO capping in the HEPES buffer solution at pH 3.0 at the excitation wavelength of 472 nm.

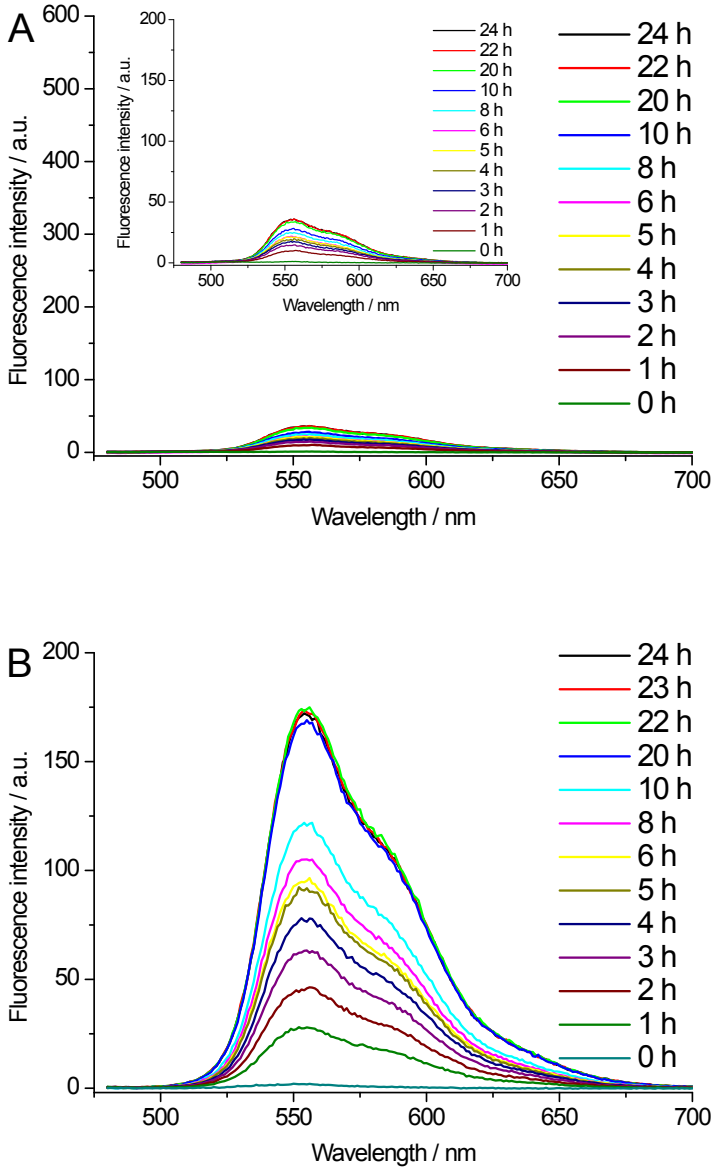

Fig. S13 Time-dependent fluorescence spectra of DOX from the ZnO-gated HMSS12 system in the HEPES buffer solutions at pH 7.4 at the excitation wavelength of 472 nm: (A) premature release; (B) GSH (10 mM)-triggered controlled release; (C) DTT (10 mM)-triggered controlled release.

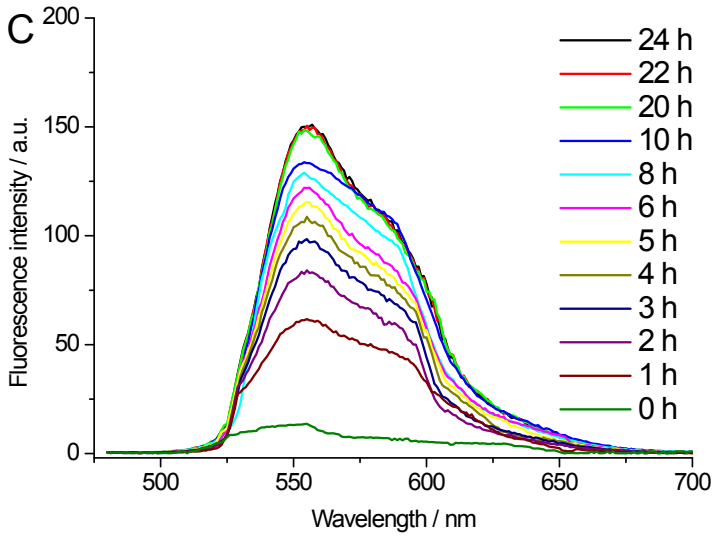

Fig. S13 (continued)

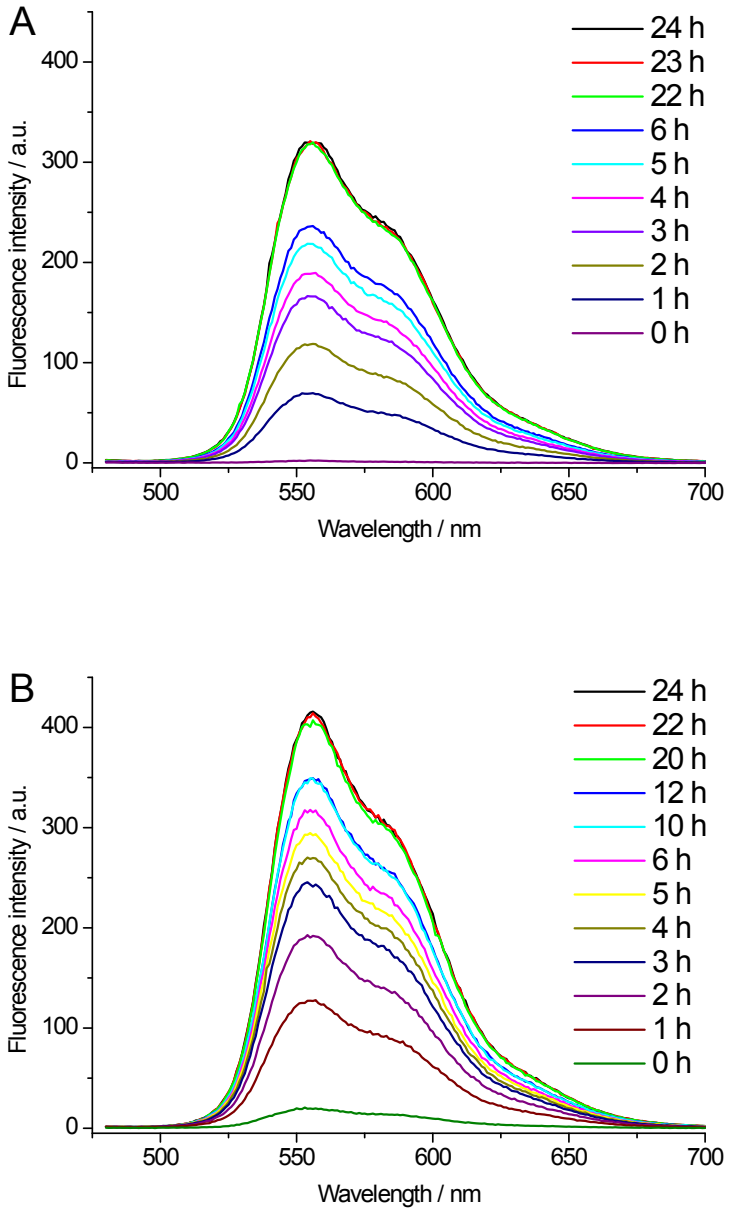

Fig. S14 Time-dependent fluorescence spectra of DOX from the ZnO-gated HMSS12 system in the presence of GSH (10 mM) in the HEPES buffer solutions at different pH at the excitation wavelength of 472 nm: (A) pH 6.0; (B) pH 5.0.